

Task-driven intra- and interarea communications in primate cerebral cortex

Adrià Tauste Campo¹, Marina Martinez-Garcia¹, Verónica Nácher², Ranulfo Romo^{2,3},
and Gustavo Deco^{1,4}

¹Center for Brain and Cognition, Department of Information and Communication Technologies,
Universitat Pompeu Fabra, 08018 Barcelona, Spain

²Instituto de Fisiología Celular-Neurociencias, Universidad Nacional Autónoma de México, 04510
Mexico D.F., Mexico

³El Colegio Nacional, 06020 Mexico D.F., Mexico

⁴Institució Catalana de Recerca i Estudis Avançats, Passeig Lluís Companys, 23, 08010 Barcelona,
Spain

Abstract

Neural correlations are central to study brain information processing and computation, and yet they have been barely analyzed due to the limited availability of simultaneous recordings. In the present work we analyzed neural correlations using spike-train recordings that were simultaneously recorded in sensory, premotor, and motor areas of a monkey during a somatosensory discrimination task. Upon modeling spike-trains as binary time series we used a non-parametric Bayesian method to estimate pairwise directional correlations between every neuron pair during the different stages of the task, namely, perception, working memory, decision making and motor action. We find that solving the task involves feed-forward and feedback correlation paths linking sensory and motor areas during certain task intervals. Specifically, task information is communicated by decision-driven neural correlations that are significantly delayed across secondary somatosensory cortex, premotor and motor areas when decision making takes place. Crucially, when the monkey is no longer requested to perform the task, the majority of these correlations consistently vanish across all areas.

1 Introduction

The problem of neural communication in the brain has been traditionally little explored due to the need of simultaneous recordings [1]. The existence of new techniques to record neural population activity and single-neuron action potentials offers new openings to study this problem [2, 3]. Recently, population recordings have motivated a large number of works on multi-

unit interactions, including the study of interactions between local field potentials (LFP) [4–6]; LFP and multi-unit activity (MUA) [5]; and LFP and neuronal spikes [7] but lesser attention has been paid at interactions between single-unit recordings [8]. Yet, the analysis of simultaneous spike trains becomes critical as it is generally assumed that neurons are key units in distributing information across brain areas [9].

An ideal paradigm to study neural communication is the somatosensory discrimination task designed by Romo et al. [10]. In this task a trained monkey discriminates the difference in frequency between two mechanical vibrations delivered sequentially to one fingertip (Fig. 1A). Crucially, the monkey must hold the first stimulus frequency (f_1) in working memory, must compare the second stimulus frequency (f_2) to the memory trace of f_1 to form a decision of whether $f_2 > f_1$ or $f_2 < f_1$, and must postpone the decision until a sensory cue triggers the motor report [11]. At the end of the task the monkey is rewarded with a drop of liquid for correct discriminations. A previous work on this task has analyzed how single-neuron responses across sensory and motor areas linearly correlate with stimuli and the decision report during the key stages of the task [12]. The results show that stimuli are mostly encoded in somatosensory areas, the processes of working memory and comparison take place in the secondary somatosensory area (S2) and premotor areas and behavioral information is primarily found in premotor and motor areas. Thus, the somatosensory discrimination task activates complex processes which require to communicate information from the areas that encode the stimuli to the areas that integrate them and report the decision.

In the present work, we study this communication paradigm through the analysis of simultaneous recordings of neurons engaged in the task [6, 13]. Indeed, by applying non-linear statistical methods we estimate modulated cortical correlations that help describe how task-related information flows from sensory to motor areas when a correct decision is made.

2 Results

We studied interactions between neuronal spike trains that were simultaneously recorded from five cortical areas in a trained monkey performing a somatosensory discrimination task [6] (*Materials and Methods*). Recordings were performed in 15 independent sessions ($n = 15$). During each session, up to seven microelectrodes were individually inserted in each of the five cortical areas for simultaneous recordings of single neurons. The selected neurons were from two somatosensory areas, primary somatosensory cortex (S1) and secondary somatosensory cortex (S2), and three premotor/motor areas: medial premotor cortex (MPC), dorsal premotor cortex (DPC) and primary motor cortex (M1). To investigate neural correlations during the discrimination task, we only considered correct (“hit”) trials of similar psychophysical performance (*Materials and Methods*).

The central measure of our analysis is the directed information (DI), mathematically de-

noted by $I(X^T \rightarrow Y^T)$, which is a non-linear measure of directional correlation between the processes X^T and Y^T [14] (*S.I.*). When the two processes are identical, i.e., $X^T = Y^T$, this measure coincides with the Shannon entropy, denoted by $H(Y^T)$ [15]. The directed information $I(X^T \rightarrow Y^T)$ quantifies for any given time t the information that the past and present of X^T (up to time t) has about the present of Y^T upon the knowledge of the past of Y^T (up to time $t - 1$). Alternatively, the entropy of Y^T quantifies the uncertainty on any realization of Y^T .

2.1 Neural correlations are task driven

We estimated the entropy in 531 neurons and the directed information in 17564 neuron pairs to infer significant auto- and pairwise directional correlations during 17 consecutive task intervals of 0.5s, spanning from the interval prior to the *f1* stimulation to the interval after the lift of the sensory cue, which will be thereafter named *pu* (probe-up) period (Fig. 1A, *Materials and Methods*). In particular, for every task interval we tested the significance of each estimated measure against a null hypothesis of complete directional independence using the maximum value of the directed information over all preselected delays as a test statistic (*Materials and Methods*). Every significant correlation (permutation test, $\alpha = 5\%$) under at least one of the frequency pairs was denoted a *responsive path* and each correlated neuron was denoted either a *starting point* or an *endpoint* neuron according to the correlation’s directionality. In a similar vein, every neuron with a significant autocorrelation was denoted a *responsive neuron*. For every interarea comparison, we computed the percentage of responsive paths over all possible simultaneous pairs. Fig. S1 shows that responsive paths were found above significance level ($\alpha' = 9.75\%$, Fig. S1) across all area pairs and task intervals (green curves).

We studied whether responsive paths were directly associated with the discrimination task. To this end, we estimated again the directional correlation in every neuron pair that formed a responsive path during a control task, in which the monkey received identical mechanical vibrations but was requested to remain still upon a reward that arrived at variable time (passive stimulation, Fig. 1A, *Materials and Methods*). Under passive stimulation, only a small fraction of the responsive paths were again found significant (20–25%) across all area pairs and task intervals (grey curves, Fig. S1). Overall, there was a low correlation between the presence of responsive paths during the original and the control task ($\rho = 0.0239$, Spearman correlation [16]) suggesting that neural correlations were driven by weakly dependent processes.

We then wondered whether both tasks were also differentiated by single-neuron measures under fixed stimulation. To examine this question, we focused on the ensemble of neurons that were endpoint neurons of responsive paths and measured their activity during each task. First, we measured the firing rate and spike-train entropy of every neuron in the ensemble. Then, as a benchmark multi-neuron measure, we evaluated the aggregated sum of directed

information along every neuron’s incoming responsive paths. Fig. 2 shows the average firing rate, average entropy and average incoming directed information during both tasks when ($f1 = 14, f2 = 22$)Hz together with their error bars. Neurons exhibited consistent single-neuron differences across tasks in MPC, DPC and M1 around $f2$ stimulation. In contrast, the use of directional correlations shows that in those periods where neurons were equally firing in both tasks (or with similar spike-train entropies) they were less influenced through responsive paths during passive stimulation than during somatosensory discrimination. Results were similar for the frequency pair ($f1 = 30, f2 = 22$)Hz (Fig. S2).

2.2 Neural correlations are modulated by decision making

Despite being task-driven, the role of responsive paths still remained unclear as they were uniformly present across all areas and task intervals (Fig. S1). In particular, to what extent were these paths communicating task information?

To investigate more intrinsic connections between neural correlations and decision making we searched for the subset of responsive paths that were significantly modulated by a task variable. Specifically, we tested the modulation of every responsive neuron and path with respect to the decision sign $D = f1 - f2$ by computing the difference between the directed information estimates across trials recorded at frequency pairs ($f1 = 14, f2 = 22$)Hz ($D < 0$) and ($f1 = 30, f2 = 22$)Hz ($D > 0$). Responsive neurons and paths that were significantly modulated (permutation test, $\alpha = 5\%$) were denoted *modulated neurons* and *modulated paths* respectively. By this choice of trials modulated paths have a different interpretation depending on the task interval. For instance, during the intervals prior to $f2$ stimulation, modulations can be regarded as correlates of $f1$ whereas during the intervals after $f2$ stimulation, they can be interpreted as correlates of the decision sign (D) and the associated motor action. Green curves in Figs. 3 and S3 show the percentage of modulated neurons (Fig. 3A) and modulated paths (Figs. 3B and S3) while the monkey was performing the discrimination task and black circles indicate the intervals where this percentage was significantly different (Agresti-Coull confidence interval [17], $\alpha = 5\%$) from significance level ($\alpha = 5\%$). Area comparisons in Fig. 3 were chosen to describe the chain of comparisons $S1 \leftrightarrow S2 \leftrightarrow MPC \leftrightarrow DPC \leftrightarrow M1$. In general, Figs. 3 and S3 show that the directional measure was able to discriminate top-down from bottom-up interactions in each recorded area pair.

As both modulated neurons and paths carried task information, we analyzed their mutual relationship by computing the proportion of modulated paths that linked modulated neurons (Fig. S4). In contrast to responsive paths, modulated neurons were positively correlated with the presence of an own outgoing or incoming modulated path (Spearman correlation, $p < 0.0001$, Fig. S4A) which implied that for every area and the majority of task intervals the proportion of modulated paths linking modulated neurons was above chance level (Fig. S4B).

This preliminary result indicates that modulated paths were prone to link encoding neurons.

Figs. 3 and S3 illustrate how sensory information was encoded and distributed from sensory to motor areas while the percept was processed to drive a motor action. To begin with, S1 encoded $f1$ at the first stimulation period and was specially active in distributing this information towards S2, MPC and M1 during working memory intervals (Figs. 3 and S3). Besides, S1 was highly interactive with premotor and motor areas around the pu period, which suggests that the sensory cue delivered at the pu period produced sensory-motor correlations that could anticipate the report (Fig. S3). In sum, S2 was more interactive during the first stimulation and working memory periods than during the postponed decisions (Fig. S3). In particular, neurons from S2 were influenced by MPC neurons according to $f1$ (Fig. 3B) without individually encoding this information (Fig. 3A). The reduced activity of S2 may be due to the fact that S2 was particularly prone to encode and integrate $f2$ [12], whose value was kept fixed in our setting. The role of MPC was to mediate between sensory and motor areas in two different stages. First, during the intervals prior to $f2$ stimulation MPC received incoming interactions from sensory areas that were modulated by $f1$ (Figs. 3B and S3). Second, during the postponed decision, MPC mainly produced outgoing interactions to M1 and to other neurons within MPC that were modulated by the decision sign (Fig. S3). Neurons from DPC were not shown to neither encode $f1$ nor the monkeys' choice. However, they shared this information among themselves and with other areas during the first stimulation and the pu period (Fig. S3). Interestingly, DPC only traced the task through a feedback path from M1 that remained active along the task. M1 presented three differentiated activity patterns. First, it was influenced by S1 around $f1$, $f2$ stimulation and probe up periods (Fig. S3), which indicates that there was a persistent information link between sensory and motor areas regardless of the encoding patterns found in each area (Fig. 3A). Second, it produced feedback paths to S1, S2 and DPC during the interstimulus interval that could be involved in fixing $f1$ in working memory. Finally, M1 was highly interactive with the rest of premotor and motor areas in the process of conforming the decision and the motor action in line with previous results [12].

In contrast, during passive stimulation neither modulated neurons nor modulated paths were in general associated with $f1$ and the monkey's choice. Modulated neurons and paths were slightly persistent in S1 during the first stimulation, in M1 during intervals post $f2$ stimulation and across both somatosensory areas before $f2$ stimulation (grey curves, Figs. 3 and S3). These traces of information suggest the existence of minimal sensory processing in S1 and S2 as well as evoked motor activity in M1 during the control task.

2.3 Sign-specific delayed correlations distribute task information

We further studied interarea communications by analyzing two characteristics of modulated paths: their modulation rule and their correlation delay. First, we divided modulated paths into three classes: ON-ON, defined to involve significant correlations in both decision signs, and ON-OFF and OFF-ON, defined to be significant only for $f1 < f2$ and $f1 > f2$ respectively. The majority of modulated paths were of the form ON-OFF and OFF-ON (Fig. 4A) indicating that task information was mainly encoded by the presence of *sign-specific* correlations, i.e., correlations that were consistently significant for one decision report but were not for the opposite. The almost equal contribution of ON-OFF and OFF-ON modulations along the task gave rise to an overall picture that was difficult to interpret (Fig. S5). To observe how these modulations interplayed for a specific interarea comparison, Fig. 4B shows the percentage of modulation classes above significant level ($\alpha = 5\%$) and Fig. 4C shows the sum of the average (across trials) directed information along modulated paths starting at M1 and ending at DPC in each decision report. Figs. 4B and 4C also highlight the three stages where the percentage of modulation paths was significantly different from the false positive rate (regions in dashed rectangle). These stages may be linked to the acquisition of $f1$ (intervals 2 and 3), the recovery of $f1$ before the comparison takes place (interval 9) and the process of planning the action (intervals 14 and 15). Comparison of both figures at the later stage shows that similar number of sign-specific paths (8-10%) could lead to different aggregated directed-information values for each decision ($\approx 1:2$ proportion).

To study interneuronal delays we divided modulated paths into three sets, 0ms, [10, 70]ms and [80, 140]ms, where the whole range was chosen to be compatible with the latency of each area [18]. We first plotted the distribution of delays across area pairs and task intervals where modulated paths were above significant level (Fig. S6, $\alpha = 5\%$). Fig. 5 resumes these findings by analyzing interneuronal delays according to the function (somatosensory/premotor/motor) and location (right/left hemisphere) of each area under comparison. Overall, modulated paths across somatosensory areas were dominated by instantaneous interactions while modulated paths involving premotor and motor areas were mostly delayed at the range [80 – 140]ms (Fig. 5A). In particular, we tested the average delay across area pairs and obtained significant differences (Fig. 5B, Wilcoxon test [16], $p < 0.005$) between somatosensory interactions (46.3ms), interactions between S1, and MPC, DPC and M1 (67.3ms), and interactions across S2, MPC, DPC and M1 (74.6ms). These differences also remained significant between the first (81.4ms) and the third (88.9ms) group when we removed the contribution of instantaneous correlations (Fig. 5C, $p < 0.05$). Further, a closer look at Fig. S6 revealed that modulated paths within the somatosensory cortex were specially faster before $f2$ stimulation than interactions across premotor and motor areas after $f2$ stimulation. These findings suggested that differences in the average delay were driven by the location of the areas in the two hemispheres. Then, we

computed the average delay across areas within a hemisphere and across areas from distinct hemispheres obtaining significant differences that were robust to the effect of intraarea correlations (Fig. 5B, $p < 0.005$). These differentiated pattern remained significant after removing the effect of instantaneous correlations (Fig. 5C, $p < 0.05$). In sum, modulated paths across opposite hemispheres involving S2, MPC, DPC and M1 were more likely to describe a direct communication link between neurons than the rest of interactions.

3 Discussion

Using a novel method to estimate directional dependencies between spike trains, we have unraveled neural correlation paths that are specific to a discrimination task. These paths are task-driven for two main reasons. First, they dramatically decrease when the monkey receives both stimuli but is not requested to perform the cognitive task (Fig. 2). Second, they are modulated in a significant percentage by sensory and behavioral variables (Fig. 3). More importantly, these modulated paths are related to neurons that individually encode task variables and are therefore likely to further distribute their information across other areas (Fig. S4). In general, the use of directional correlations seems to better discriminate the original task from a control task than single-neuron measures (Fig. 2A) suggesting that task-driven correlations may not be in general rate dependent [19].

Modulated paths can be used to further characterize the role of each area while solving the task [11, 12]. In particular, we observed that S1 is particularly important in feed-forwarding sensory information to superior areas, S2 interacts with MPC during the working memory stage, MPC acts as a relay node between sensory and motor areas and the interactions across $MPC \leftrightarrow M1 \rightarrow DPC$ concentrate the information on the monkey's choice (Figs. 3 and S3). Modulated paths mainly encode task information by the existence (ON) and absence (OFF) of a given neural correlation, which indicates that each decision is internally mapped to a different subset of interactions (Fig. 4). For each decision report, modulation paths are delayed according to the hemisphere location and function of each area under comparison. In particular, modulated paths are significantly faster when they distribute information across somatosensory areas (S1 and S2) during intervals prior to the f2 stimulation than when they link S2, premotor and motor areas during decision making. This indicates that sensory and behavioral information may be communicated at different time scales.

Our description of communication paths in primate cerebral cortex extends beyond previous works in which task-related activity was found to be highly distributed across areas and time intervals [12]. To encompass both sets of results, we make hypotheses in two related directions. On one hand, our analysis of modulation paths suggests that task-related information is jointly encoded by neurons that often do not exhibit individual modulations. On the other, the great percentage of responsive paths that are not modulated indicates that

there is context-dependent activity beyond encoding of sensory and behavior variables (f_1 , f_2 and decision). This activity may be the result of internal processes involving sensory and motor areas such as arousal, attention or motivation [20] whose encoding patterns could not be captured with this experimental paradigm. The study of these hypotheses may shed light on the underlying coding mechanism that encodes and distributes the required information to solve a cognitive task.

4 Materials

This study was performed on one adult male monkey (*Macaca mulatta*), weighing 12 kg. All procedures followed the guidelines of the National Institutes of Health and Society for Neuroscience. Protocols were approved by the Institutional Animal Care and Use Committee of the Instituto de Fisiología Celular.

4.1 Recordings

Data acquisition, amplification, and filtering were described in detail [10]. In brief, the activity of single neurons were simultaneously recorded with an array of seven independent, movable microelectrodes (1-1.5 M Ω) inserted in each of five cortical areas. Electrodes within an area were spaced 305 or 500 μm apart [21]. Spike sorting was performed manually on-line, and single neurons were selected if they responded to any of the different components of the discrimination task [10,12]. The cortical areas were the S1, S2, MPC, DPC, and M1 (Fig. 1B). Recordings in S1, S2, and DPC were made in the hemisphere contralateral to the stimulated hand (left hemisphere), and in MPC and M1 contralateral to the responding hand/arm (right hemisphere).

4.2 Discrimination Task

The paradigm used here has been described [10,11]. The monkey sat on a primate chair with its head fixed in an isolated, sound- proof room. The right hand was restricted through a half-cast and kept in a palm-up position. The left hand operated an immovable key (elbow at $\sim 90^\circ$), and two push buttons were in front of the animal, 25cm away from the shoulder and at eye level. The centers of the switches were located 7 and 10.5cm to the left of the midsagittal plane. In all trials, the monkey first placed the left hand and later projected to one of the two switches. Stimuli were delivered to the skin of the distal segment of one digit of the right, restrained hand, via a computer-controlled stimulator (2mm round tip; BME Systems). The initial probe indentation was 500 μm . Vibrotactile stimuli were trains of short mechanical pulses. Each of these pulses consisted of a single- cycle sinusoid lasting 20ms. Stimulus amplitudes were adjusted to equal subjective intensities; for example, 71 μm at 12Hz

and $51\mu\text{m}$ at 34Hz (a decrease of $\sim 1.4\%$ per Hz). During discrimination trials (Fig. 1A), the mechanical probe was lowered (probe down; pd), indenting the glabrous skin of one digit of the hand; the monkey placed its free hand on an immovable key (key down; kd); after a variable prestimulus delay ($0.5 - 3\text{s}$) the probe oscillated vertically at the frequency of the first stimulus ($f1$); after a fixed delay (3s), a second mechanical vibration was delivered at the second stimulus ($f2$) frequency; after another fixed delay (3s) the probe is lifted off from the skin (probe up; pu); the monkey released the key (ku) and pressed either a lateral or a medial push button (pb) to indicate whether $f2$ was of higher or lower frequency than $f1$, respectively. The monkey was rewarded with a drop of liquid for correct discriminations.

4.3 Control tests

Passive stimulation. During this condition, the monkey was trained to maintain its free arm motionless during the trial (Fig. 1B). Stimuli were delivered to the fingertip and the animal remained alert by being rewarded with drops of liquid at different times, but no motor response with the free hand was required.

4.4 Data analysis

Data were analyzed offline by using custom-build Matlab code (MathWorks). We selected 15 populations of neurons with approximately 40 neurons per area. We estimated neural directional correlations between every neuron pair within a population using a non-parametric estimator of the directed information between a pair of discrete time series [22]. Specifically, for a pair of time series (x^T, y^T) , the directed information between the underlying stationary processes \mathcal{X} and \mathcal{Y} is estimated via the formula

$$\hat{I}(\mathcal{X} \rightarrow \mathcal{Y}) = \frac{1}{T} \sum_{t=1}^T \sum_{y_t} \hat{P}(Y_t = y_t | X^t = x^t, Y^{t-1} = y^{t-1}) \times \log \frac{\hat{P}(Y_t = y_t | X^t = x^t, Y^{t-1} = y^{t-1})}{\hat{P}(Y_t = y_t | Y^{t-1} = y^{t-1})}, \quad (1)$$

where the conditional probabilities $P(\cdot | X^t = x^t, Y^{t-1} = y^{t-1})$ are estimated using the context-tree weighting method [23]. This estimator is consistent as long as $(\mathcal{X}, \mathcal{Y})$ forms a jointly stationary irreducible aperiodic finite-alphabet Markov process whose order does not exceed the prescribed maximum depth in the CTW [22, Th. 3]. To estimate the directed information we preprocessed our data as follows. For a fixed stimulation pair, we first binarized spike-train trials using bins of 2ms (mapping 1 to each bin with at least one spike and 0, otherwise). We then divided each time series into 17 consecutive task intervals of 0.5s (250 bins). For each neuron, segments which corresponded to the same type of trials and task interval were

assumed to be generated by a common process that satisfied the estimator requirements with a maximum memory of 4ms (2 bins). Then, for each neuron pair and task interval, we run the directed information estimator over a pair of time series, which individually resulted from the concatenation of these segments. We repeated the same procedure to estimate causal correlations at delays $\delta \in [0, 140]$ ms in steps of 10ms (S.I.).

To assess the statistical significance of the estimations we used a Monte-Carlo permutation test [24], where the original (i.e., non permuted) results were compared with the tail of a distribution obtained by permuting 20 times the concatenations of the second binarized spike train Y^T differently for each original estimation ($\alpha = 5\%$) and computed the corresponding p-value [25]. We dealt with the multiple test problem (one test for each delay) by using the maximum directed information over all preselected delays as a test statistic. Further details about the significance analysis for the directed information computations and the modulation tests are provided in the S.I. (Sec. 4).

5 Acknowledgments

R.R.'s research was partially supported by International Research Scholars Award 55005959 from the Howard Hughes Medical Institute, Dirección de Personal Académico de la Universidad Nacional Autónoma de México Grant IN203210 and Consejo Nacional de Ciencia y Tecnología Grant CB-2009-01-130863. V.N. was supported by a Ministerio de Educación y Ciencia (MEC)-Fullbright Postdoctoral Fellowship from the Spanish Ministry of Science and Technology and Dirección de Personal Académico de la Universidad Nacional Autónoma de México. Support for this work was provided by European project Brainscales (to G.D. and M.M.-G). In addition, G.D. was supported by the ERC Advanced Grant: DYSTRUCTURE (n. 295129), by the Spanish Research Project SAF2010-16085. A.T.C. was supported by the European Community's Seventh Framework Programme (FP7/2007-2013) under grant agreement PEOPLE-2012-IEF-329837.

References

- [1] Salinas E, Sejnowski T (2001) Correlated neural activity and the flow of information. *Nat Rev Neurosci* 2(8):539-550.
- [2] Brown EN, Kass RE, Mitra PP (2004) Multiple neural spike train data analysis: state-of-the-art and future challenges. *Nat Neurosci* , 7(5):456-461.
- [3] Buzáki G (2004) Large-scale recording of neuronal ensembles. *Nat neuroscience*, 7(5):446-451.

- [4] Roelfsema PR, Engel AK, Konig P, Singer W (1997) Visuomotor integration is associated with zero time-lag synchronization among cortical areas. *Nature*, 385:157-161.
- [5] Womelsdorf T, et al. (2007) Modulation of neuronal interactions through neuronal synchronization. *Science*, 316(5831):1609-1612.
- [6] Nácher V, Ledberg A, Deco G, Romo R (2013) Coherent delta-band oscillations between cortical areas correlate with decision making. *Proc Natl Acad Sci USA* 110(37):15085-90.
- [7] Koralek AC, Costa RM, Carmena JM (2013) Temporally precise cell-specific coherence develops in corticostriatal networks during learning. *Neuron*, 79(5):865-872.
- [8] Hoffman KL, McNaughton BL (2002) Coordinated reactivation of distributed memory traces in primate neocortex. *Science*, 297(5589):2070-2073.
- [9] Kolb B, Whishaw IQ (2001) *An introduction to brain and behavior*. Worth Publishers.
- [10] Hernández A, Salinas E, García R, Romo R (1997) Discrimination in the sense of flutter: New psychophysical measurements in monkeys. *J Neurosci* 17(16):6391-6400.
- [11] Lemus L, et al. (2007) Neural correlates of a postponed decision report. *Proc Natl Acad Sci USA* 104(43):17174-17179.
- [12] Hernández A, et al. (2010) Decoding a perceptual decision process across cortex. *Neuron* 66(2):300-314.
- [13] Hernández A, et al. (2008) Procedure for recording the simultaneous activity of single neurons distributed across cortical areas during sensory discrimination. *Proc Natl Acad Sci USA*, 105(43):16785-90.
- [14] Massey J (1990) Causality, feedback and directed information. *Proc. Int Symp Inf. Theory Applic*: 303-305.
- [15] Shannon C, Wiener W (1949) *The mathematical theory of communications*. Univ of Illinois Press.
- [16] Kendall MG (1948) *Rank correlation methods*.
- [17] Agresti A, Coull BA (1998) Approximate is better than “exact” for interval estimation of binomial proportions. *The American Statistician*, 52(2):119-126.
- [18] de Lafuente V and Romo R (2006) Neural correlate of subjective sensory experience gradually builds up across cortical areas. *Proc Natl Acad Sci USA* 103(39):14266-71.

- [19] de la Rocha J, Doiron B, Shea-Brown E, Josic K, Reyes A (2007) Correlation between neural spike trains increases with firing rate. *Nature* 448(7155):802-806.
- [20] Cohen MR, Kohn A (2011) Measuring and interpreting neural correlations. *Nat Rev Neurosci* 14(7):811-819.
- [21] Eckhorn R, Thomas U (1993) A new method for the insertion of multiple microprobes into neural and muscular tissue, including fiber electrodes, fine wires, needles and micro-sensors. *J Neurosci Methods* 49(3):175-179.
- [22] Jiao J, Permuter H, Zhao L, Kim K, Weissman T (2013) Universal estimation of directed information. *IEEE Trans Inf Theory* 59(10):6220-6242.
- [23] Willems F, Shtarkov Y, Tjalkens T (1995) The context-tree weighting method: Basic properties. *IEEE Trans. Inf. Theory*, 41(3):653-664.
- [24] Ernst M (2004) Permutation methods: A basis for exact inference. *Stat Sci* 19(4):676-685.
- [25] Phipson B and Smyth GK (2010) Permutation p-values should never be zero: calculating exact p-values when permutations are randomly drawn. *Stat Appl in Gen and Molec Bio* 9:346-382.

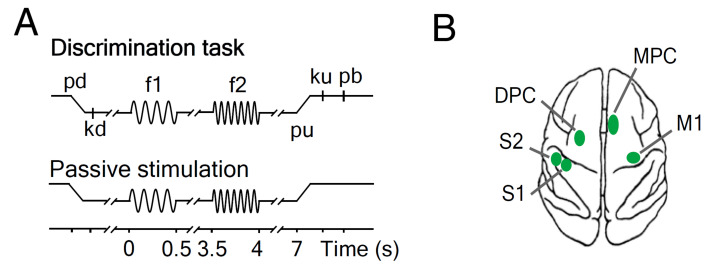


Figure 1: Somatosensory discrimination task and cortical recoding sites. (A) Sequence of events during the discrimination and the passive stimulation tasks ($f1$, first stimulus; $f2$, second stimulus; kd , key down; ku , key up; pb , push button; pd , probe down; pu , probe up; (*Materials and Methods*). (B) Top view of the monkey brain and the recorded cortical areas (green spots). S1, primary somatosensory cortex; S2, secondary somatosensory cortex; MPC, medial premotor cortex; DPC, dorsal premotor cortex; M1, primary motor cortex.

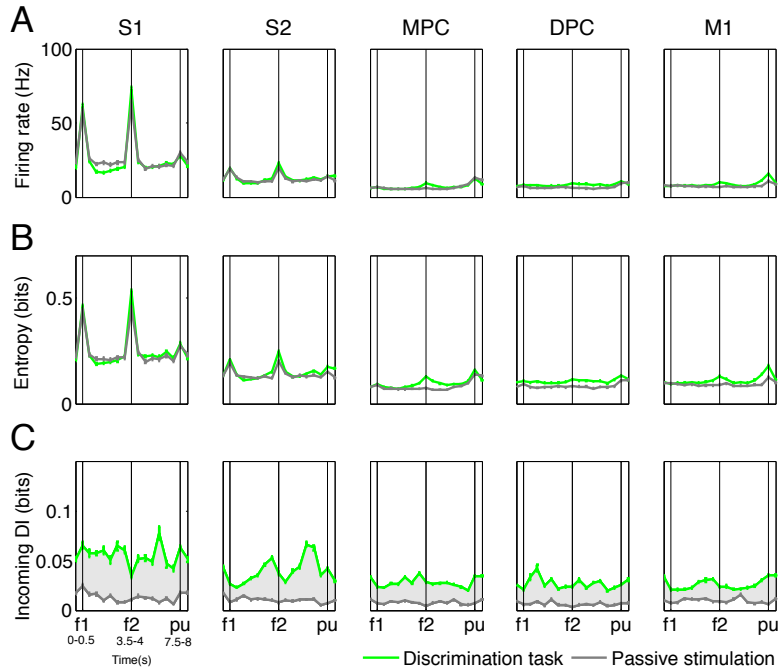


Figure 2: Single-neuron vs. multiple-neuron measures. Comparison between discrimination (green) and passive stimulation tasks (grey) across areas using the average value of distinct measures over the ensemble of neurons with incoming responsive paths. Data was obtained in 15 sessions ($n = 15$) from areas S1, primary somatosensory cortex; S2, secondary somatosensory cortex; DPC, dorsal premotor cortex; MPC, medial premotor cortex; M1, primary motor cortex, and is plotted for 17 consecutive intervals when $f1 = 14\text{Hz}$ and $f2 = 22\text{Hz}$. Vertical bars outline the intervals $f1$, $f2$ and pu period. Error bars (\pm SEM) denote the standard deviation of each measure. (A) Average firing rate. (B) Average entropy. (C) Average (across the ensemble of neurons) sum of directed information (DI) along incoming responsive paths. The shadowed grey area indicates the difference of this measure between both tasks.

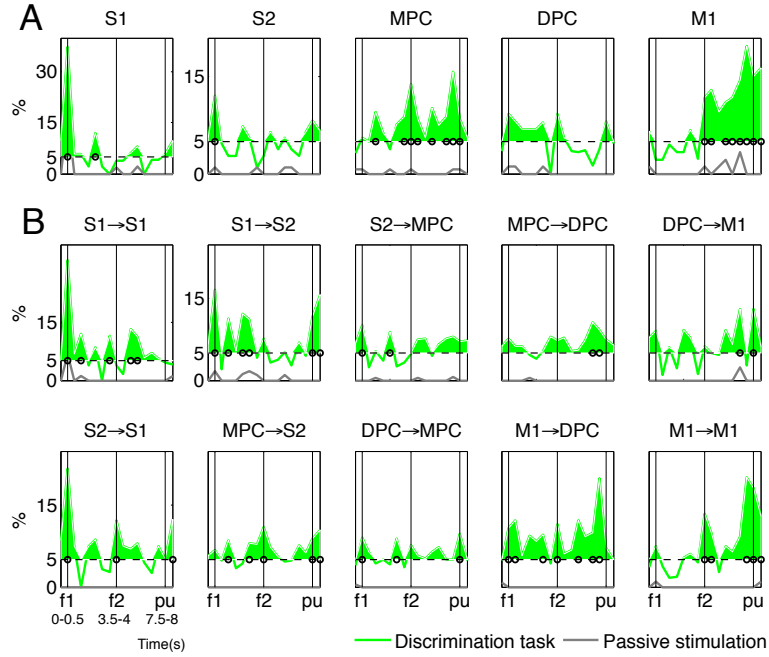


Figure 3: Modulated neurons and paths. In green, percentages during the discrimination task. In grey, percentages during passive stimulation. Arrows in the title indicate the directionality of the modulated paths. Vertical bars outline the intervals $f1$, $f2$ and pu period. Horizontal dashed lines indicate significance level $\alpha = 5\%$. The shadowed green area indicates the percentages of modulated paths above significance level. Black circles indicate the intervals where the estimated percentage was significantly different (Agresti-Coull confidence interval [17], $\alpha = 5\%$) from significance level. (A) Percentage of modulated neurons over all responsive neurons in each recorded area. (B) Percentage of modulated paths over all responsive paths in 10 intra- and interarea comparisons. Data was obtained in 15 sessions ($n = 15$) from areas S1, primary somatosensory cortex; S2, secondary somatosensory cortex; DPC, dorsal premotor cortex; MPC, medial premotor cortex; M1, primary motor cortex, and is plotted for 17 consecutive intervals.

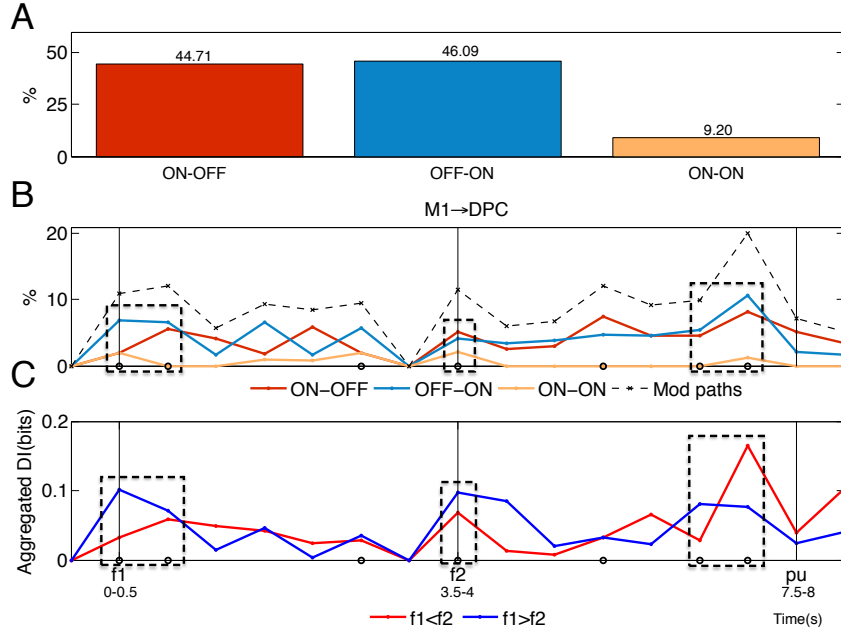


Figure 4: Modulation classes during the discrimination task. (A) Distribution of modulated paths from intervals above significant level ($\alpha = 5\%$) into the classes ON-OFF, OFF-ON and ON-ON. (B) For the comparison MPC-DPC, percentage of modulation classes during task intervals above significant level: percentages of ON-OFF modulations (significant only for $f_1 < f_2$, red), percentages of OFF-ON modulations (significant only for $f_1 > f_2$, blue), and percentages of ON-ON modulations (significant for both decision reports, orange). For reference, the total percentage of modulated paths is plotted in a dashed black line with cross markers. (C) Aggregated sum of the average (across trials) directed information (DI) along modulated paths from MPC to DPC during task intervals above significant level for the decision reports ($f_1 = 14\text{Hz}$, $f_2 = 22\text{Hz}$), ($f_1 < f_2$, red) and ($f_1 = 30\text{Hz}$, $f_2 = 22\text{Hz}$), ($f_1 > f_2$, blue). (B)-(C) Arrows in the title indicate the directionality of the modulated paths. Vertical bars outline the intervals f_1 , f_2 and pu period. Data was obtained in 15 sessions ($n = 15$) from areas S1, primary somatosensory cortex; S2, secondary somatosensory cortex; DPC, dorsal premotor cortex; MPC, medial premotor cortex; M1, primary motor cortex, and is plotted in (B) and (C) for 17 consecutive intervals.

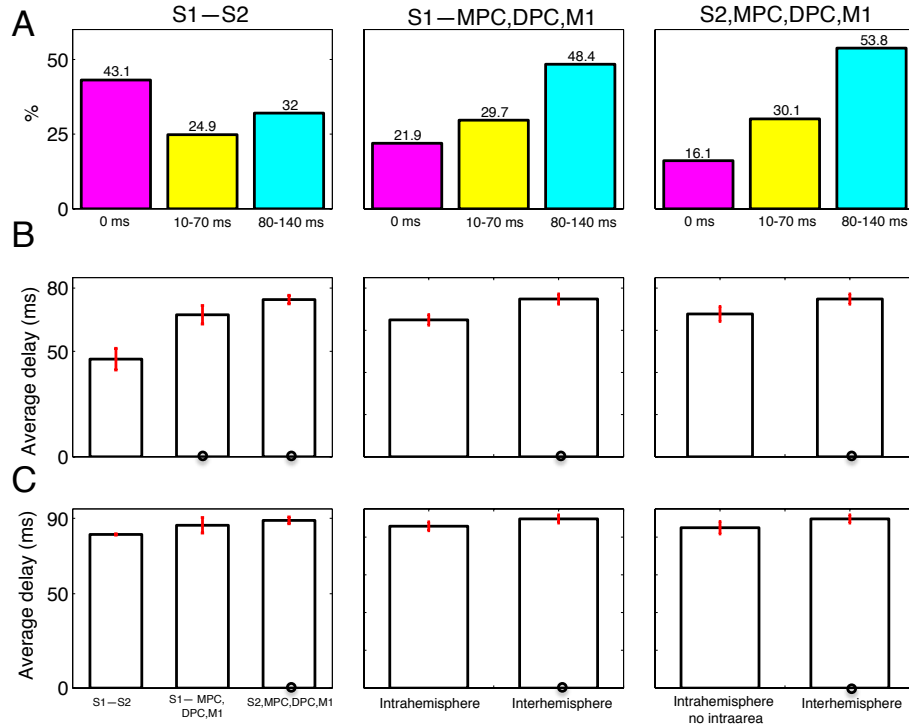


Figure 5: Interneuronal delays during the discrimination task. (A) Distribution of modulated path delays at intervals above significant level ($\alpha = 5\%$) into 0ms (magenta), 10–70ms (yellow) and 80–140ms (cyan) in correlations across S1 and S2 (left); correlations between S1 and MPC, DPC and M1 (center); and correlations across S2, DPC, MPC and M1 (right). (B)-(C) Average delay of correlations across S1 and S2; correlations between S1 and MPC, DPC and M1; and correlations across S2, DPC, MPC and M1 (left). Average delay of correlations across areas within the same hemisphere (“intrahemisphere”) and across areas from opposite hemispheres (“interhemisphere”) (center). Average delay of correlations across areas within the same hemisphere excluding correlations within the same area (“intrahemisphere no intraarea”) and across areas from opposite hemispheres (right). Error bars in red (\pm SEM) denote the standard deviation of the delays. Black circles indicate that the difference against the leftmost category was significant (Wilcoxon test, $\alpha = 5\%$). (B) Average delay of modulated paths. (C) Average delay of non-instantaneous modulated paths. Data was obtained in 15 sessions ($n = 15$) from areas S1, primary somatosensory cortex; S2, secondary somatosensory cortex; MPC, medial premotor cortex; DPC, dorsal premotor cortex; M1, primary motor cortex.